Indonesian Physical Review
Volume 08 Issue 03, September 2025
P-ISSN: 2615-1278, E-ISSN: 2614-7904

Integrating High-Resolution Gravity Gradients and 3D Inversion Modeling to Delineate Mineral Resources in the Lewa District, East Sumba, Indonesia

Aprianus Raja[1], Jehunias Tanesib[1], Laura A.S. Lapono[1], Richard Lewerissa[2*]
[1] *Department of Physics, Faculty of Sciences and Technology, Nusa Cendana University; Nusa Tenggara Timur, Kupang 85148, Indonesia*
[2] *Department of Physics, Faculty of Mathematics and Natural Sciences, Papua University; Papua Barat, Manokwari 98314, Indonesia*

Corresponding Authors E-mail: r.lewerissa@unipa.ac.id

Article Info

Article info:
Received: 01-05-2025
Revised: 23-07-2025
Accepted: 28-07-2025

Keywords:
Mineral resources, GGMplus, ERTM 2160, vertical and horizontal gradient, tilt angle, gravity modeling

How To Cite:
A. Raja, J. Tanesib, L. A.S. Lapono, and R. Lewerissa, "Integrating High-Resolution Gravity Gradients and 3D Inversion Modeling to Delineate Mineral Resources in the Lewa District, East Sumba, Indonesia", Indonesian Physical Review, vol. 8, no. 3, p 712-733, 2025.

DOI:
https://doi.org/10.29303/ipr.v8i3.501.

Abstract

Research in Lewa District, East Sumba Regency, Indonesia, aimed to identify mineral potential and clarify subsurface geological structures through gravity gradient analysis and 3D inversion modeling. This approach addresses the limitations of field gravity data in the study area. The gravity gradient method was chosen to delineate geological structure boundaries (such as formation contacts and faults) compared to conventional gravity methods and for processing global satellite data (GGMplus and EGM2008 derivatives of ERTM 2160) with limited measured data. Gravity gradient analysis, including vertical, horizontal gradient, and tilt angle, was applied to Complete Bouguer Anomaly data using 2D Fourier transformation. Gravity field correction in Lewa showed positive anomalies from volcanic basement rocks. The gradient analysis sharpened boundaries of anomalies linked to geological structures. Zero contours of vertical gradient and tilt angle defined structural boundaries, while peaks of horizontal gradient and tilt angle indicated metallic mineral sources. 3D gravity inversion modeling (density 2.22–2.97 g/cm³) showed rock intrusions at 215 meters depth, interpreted as key to mineralization formation. The 2D sections (A-A', B-B', C-C') contain Masu Formation volcanic rocks, with fault zones filled by Waikabubak Formation sedimentary rocks and silicified rocks from magma intrusion alteration. Fault systems were identified through vertical gradient extremes, representing contact formation. Highly positive contour values on the tilt angle map confirm the influence of the volcanic basement rock. Metal mineralization is closely related to tectonic activity and alteration from massive igneous intrusion. The integration of gravity gradient analysis and 3D inversion modeling has proven to be effective in mapping geological structures and identifying mineral prospects using limited data. These findings provide insights into the subsurface geology of Lewa and provide a basis for further mineral exploration in East Sumba.

Introduction

East Sumba is a regency on Sumba Island, with the capital Waingapu and an area of ± 7000 km^2 [1]. Located in southern Indonesia, it is flanked by the Salura and Manggudu Islands to the south and Nuha Island to the east (Figure 1). The region has a semi-temperate climate with annual rainfall varying from 800 to 1000 mm in the north to 1500-2000 mm [2]. The stratigraphy of Sumba Island comprises sedimentary, volcanic, and intrusive rocks, with the Praikajelu Formation being the oldest and containing graywacke flakes, lanau, clay, silt, and lime conglomerate. The East Sumba Regency contains non-metallic minerals, including limestone, coal, ocher, andesite, sirtu, batusabak, granite, basalt, diorite, calcite, quartz, sawed wood, and clay, while metallic materials include lead and iron sand [1]. Mineral systems refer to geological elements that influence the creation and maintenance of deposits. Factors include the geologic environment, drivers, mineralization timing, fluid sources and components, fluid pathways (including magma), depositional locations, and post-depositional modifications, classified as source, pathway, and location [3].

Prior research has identified the geological and mineral exploration potential and mapped the study area. In 1997, PT BHP Sumba Minerals conducted regional gold mineral exploration on Sumba Island. The study of prospects for metal mineralization has been carried out using a geochemical approach to river deposits in the East Sumba Regency. A survey on the presence of several metal minerals, such as lead and iron sand, in East Sumba was also conducted by PT Lancarjaya Bara Nusantara in 2009 [2]. Geochemical surveys conducted in the study area identified the presence of three faults and several metal anomalies, including those of silver (Ag), arsenic (As), gold (Au), lead (Pb), antimony (Sb), and zinc (Zn). The region is characterized by a complex geological structure comprising the Kananggar, Waikabubak, and Masu Formations [2]. These studies indicate the potential for hydrothermal mineralization. Nevertheless, this research relies solely on surface measurement data and does not examine subsurface structures as a source of anomalies. The geochemical anomalies observed at the surface were insufficient to confirm the source of mineralization at depth. Without an understanding of subsurface geological structures, such as faults or intrusions, it is not possible to prioritize exploration sites effectively. Therefore, further research is needed to support the identification of metal mineral potential related to subsurface geological structures in the East Sumba region, especially in the Lewa District.

Our study used the gravity method to identify this potential. The gravity method is used to assess geological structures on a large scale, although it is also applicable on a small scale to mine exploration, the environment, engineering studies, etc. [4]. This method is commonly used in the exploration of mineral resources and geological studies. The main purpose is to determine the parameters of the source, such as depth and boundary location [5]. We utilized secondary data on Earth's high-resolution gravity field by integrating the Global Gravity Model Plus (GGMplus) [6] with the Earth Residual Terrain Model (ERTM) 2160 [7]. These models were employed as substitutes owing to the lack of gravity measurement data in the study area. To identify mineral potential, we examined Earth's gravitational field gradients, including vertical and horizontal gradients and gradient ratio combinations. The directional derivative employs either the first or second vertical or horizontal gradients to amplify boundary impacts and define the boundaries between gravity and pseudo-gravity sources [8]. Horizontal and vertical gradients are necessary to improve boundary delineation in anomaly maps [9]. This study explored the qualitative interpretation of gravity anomaly maps from GGMplus and ERTM 2160 high-resolution gravity field corrections. This study focuses on

Earth's gravity gradients by analyzing the vertical, horizontal, and tilt angles of the Bouguer anomaly, employing the Fast Fourier Transformation.

To support the qualitative analysis of the Earth's gravity gradient in the Lewa district, we conducted gravity modeling through 2D forward modeling and 3D inversion modeling. Forward modeling simulates the theoretical gravity response of hypothetical geological sources, such as fault zones, based on density contrast, geometry, and depth. 3D inversion modeling of gravity data reconstructs subsurface density distribution from gravity anomalies, minimizing the error between observed and predicted anomalies. The results of this research are expected to clarify the boundaries of geological structures and specific sources of anomalies, as well as reveal the potential distribution of metallic mineral resources in the study area. This identification is the basis for more targeted, efficient, and low-cost exploration planning.

In addition, the findings of the qualitative analysis of gravity gradients serve as the main reference in 3D inversion quantitative modeling, particularly in determining the subsurface density distribution and characteristics of rock intrusions in the Lewa district. The integration of this qualitative-quantitative approach not only supports mineral exploration optimization but also contributes to the understanding of tectonic dynamics and magmatic processes that shape the geological evolution of the East Sumba volcanic region. Qualitative analysis of gravity gradients, including vertical, horizontal, and tilt angle assessments, is anticipated to delineate the boundaries of significant geological structures and mineral source zones. Quantitatively, 3D inversion modeling corroborates the presence of rock intrusions as determinants of mineralization. The integration of these methodologies offers a comprehensive understanding of the relationship between subsurface structures and the potential for metallic mineral deposits in Lewa, East Sumba.

Geological Setting

Sumba Island, in the Wallacea region between the Asian and Australian faunal groups, shows high endemicity and local fauna. Sumba Island, with its rock features, fossils, and gravity studies, was part of Sundaland and moved south during the Early Miocene [10]. During Late Miocene, Australian crust subduction beneath the Banda arc led to Sumba ridge uplift. The diachronic emergence of the Sumba ridge occurred three million years ago in the east and one million years ago at Cape Laundi, causing Quaternary coral reef development north and southern collapse. Sumba Island is located at a geological juncture where oceanic subduction occurs to the west and arc-continent collision is evident to the east.

Sumba Island is oblong, extending northwest to southeast, with four morphological units: coastal, hilly, karst, and mountainous landscapes [1]. Its geological stratigraphy includes sedimentary, volcanic, and intrusive rocks. The oldest rock, the Praikajelu Formation, is comprised of Late Cretaceous mudstones, shales, boulders, muddy marls, and clayey sandstones. In the Paleocene era, two distinct magmatic events led to the creation of the Masu Formation lavas, breccias, and intrusive rocks, which include granite, granodiorite, diorite, and syenite. The Eocene limestones of the Watopata Formation are situated above and intersect with the limestones of the Tanahroong Formation. The Paumbapa Formation consists of Oligocene reef limestones deposited unconformably. The mudstones of the mid-Miocene Pamalar Formation were deposited unconformably [10].

Mineralization here is not as intense as that in the inner Banda Arc (volcanic arc), resulting from Neogene tectonism. The mineralization cycle was influenced by Paleogene magmatism of the Sumba-Timor volcanic arc, producing andesitic volcanic rocks and andesitic intrusions in southwestern, central, and southeastern Sumba [2]. The Lewa sub-district is located on the coast of northern Sumba Island. The morphology is generally undulating, but the river walls are steep, especially in limestone areas. The river is dry, although volcanic rocks are usually watery with gradual walls. The geology consists of four rock units, from old to young: andesitic-basaltic volcanic rock units, intrusions, limestone, and sandstone (Figure 1). Geological structures appear as a morphological alignment northeast-southwest, characterized by strike-slip faults and folding structures with a moderate layer slope, cut by morphology in limestone and claystone units.

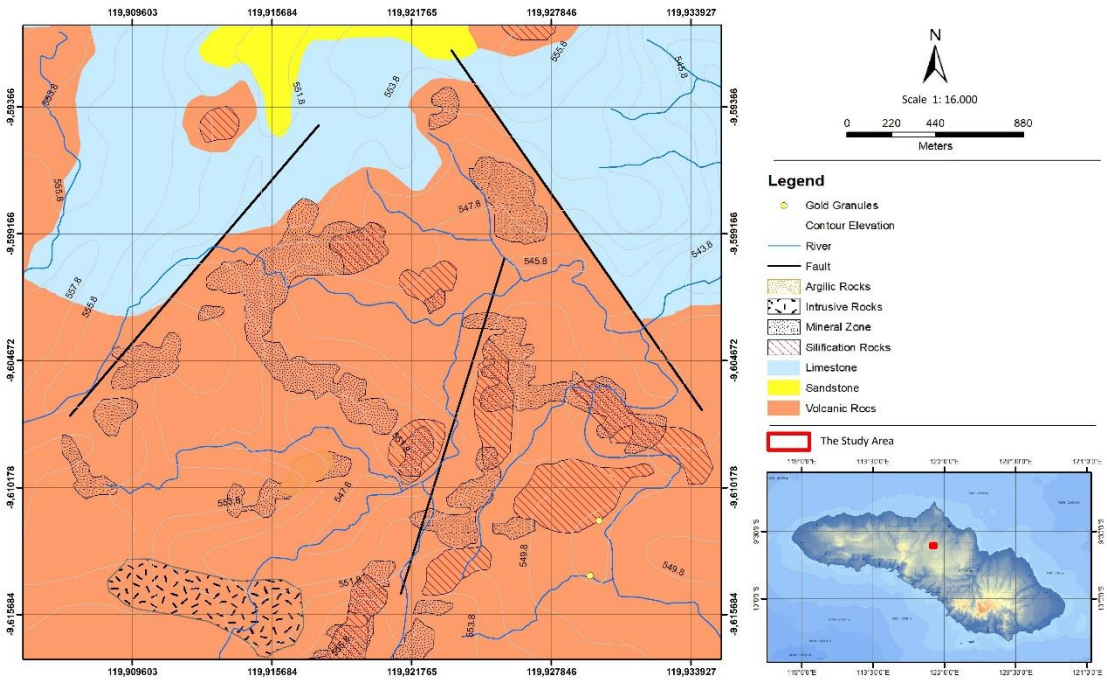

Figure 1. Geological Composite Map of Lewa District, East Sumba Regency [2].

Methods

High-resolution of Earth's gravity field

Understanding the Earth's gravity field is advantageous for exploration, geophysics related to potential fields, climate studies, and sea-front transitions [6]. Despite this, the precision of Earth's gravity field models is restricted to regional spatial scales of 2-10 km, which presents challenges in local field analysis, such as modeling water flow for engineering purposes or conducting in situ reductions in local gravitational surveys. The high-resolution of local earth gravity fields on land and archipelagos cover a region of ± 60 °latitude, as well as a spatial grid of 7.2 arcseconds (± 220 m), called GGMplus.

GGMplus serves as a valuable data source for geophysical and exploration industries, facilitating field-based analysis of comprehensive gravity measurements. This highlights promising locations for mineral exploration that do not require advanced time-reduction measurements [6]. ERTM 2160 represents a short-scale model of the Earth's gravity field,

created through gravity forward modeling utilizing data from the Global Shuttle Radar Topography Mission (SRTM). This model features a spatial scale that aligns with a harmonic spherical coefficient of 2160° and is employed to create a GGMplus gravity map covering a range of 10–250 m [7]. This study utilizes GGMplus data on Earth's gravity acceleration along with a Digital Elevation Model from ERTM 2160, covering a 5° × 5° region in Nusa Tenggara Timur (Figure 2).

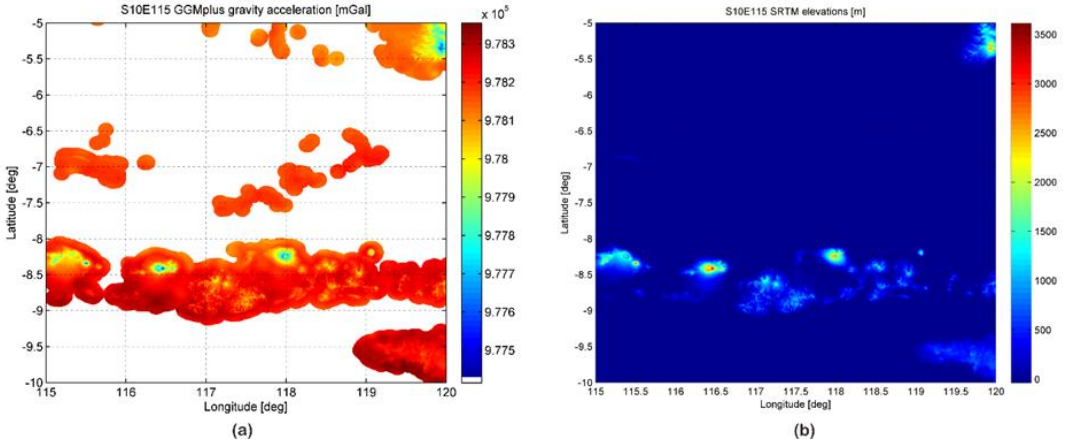

Figure 2. High-resolution Earth gravity field model in Nusa Tenggara Timur: (a) Earth gravity acceleration of GGMPlus [6] and (b) topographic elevation of ERTM 2160 [7].

Reduction of High-resolution Earth's gravity field

The research area encompasses the Lewa district in the East Sumba Regency, located in the Nusa Tenggara Timur Province of Indonesia, with coordinates ranging from 119.901 °E to 119.939 °E and 9.591 °S to 9.619 °S (Figure 3). The high-resolution Earth gravity field data reduction begins with the data extraction of GGMplus and ERTM 2160 from Curtin University, Perth, Australia, using the GNU Octave software, which is equivalent to MATLAB. The GGMplus model represents Earth's gravity acceleration (g), while ERTM 2160 serves as a DEM with 7.2 arcsecond grid spacing (± 220 m). Data processing began by ensuring that satellite data were comparable to gravity field observations collected in the study area (Table 1). We used the measurement of Earth gravity acceleration and elevation data at two airports near Lewa, including the Tambolaka and Waingapu airports, which have known gravity field references.

Table 1. Reference gravity station at Tambolaka and Waingapu Airport, Sumba Island, Nusa Tenggara Timur province.

No.	Airport	Latitude (Degree)	Longitude (Degree)	Elevation (m)	Gravity acceleration (mGal)
1	Tambolaka Waikabubak	-9.40000	119.40000	48.40	978287.54
2	Waingapu Mau Hau	-9.66667	120.30000	12.20	978295.13

To achieve a complete Bouguer anomaly, corrections were made to the GGMplus and ERTM 2160 models. In the gravity method, this adjustment is the standard. Significant anomalies include free air anomalies (FAA), simple Bouguer anomalies (SBA), and complete Bouguer anomalies (CBA). The FAA and CBA can be determined using [11]:

$$FAA = Gobs - LC + FAC \quad (1)$$

$$CBA = FAA - BC + TC \quad (2)$$

In this context, G_{obs} represents the observed gravity, *LC* denotes the latitude correction, *FAC* stands for free-air correction, and *BC* refers to the Bouguer correction. In Equation (2), the gravitational acceleration value from GGMplus is used for the observed gravity field, whereas the DEM value from ERTM 2160 is applied for both free air and Bouguer corrections.

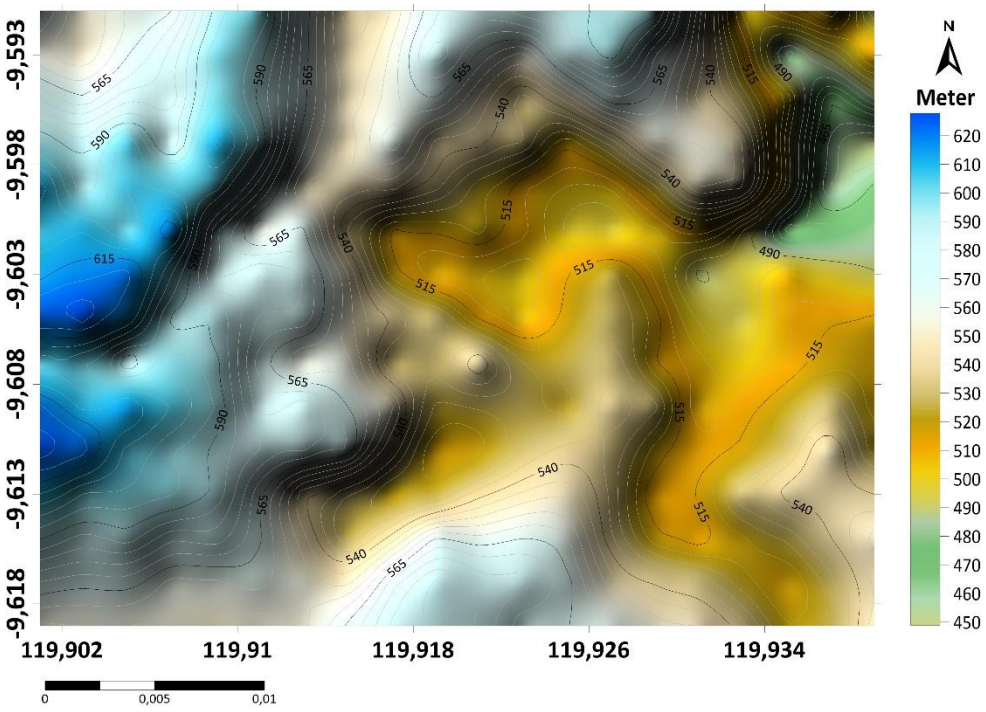

Figure 3. Research location in Lewa District, East Sumba Regency, Nusa Tenggara Timur Province, Indonesia.

In addition, we performed a spectral analysis on the CBA dataset to determine the average subsurface depth without requiring geological or density information from the area under study. The radial amplitude (A) was determined by computing the amplitude spectrum derived from the 2D Fourier transform centered at the origin (k_x = k_y = 0) with radius k_r [12]:

$$A = |F| = \sqrt{Re(F)^2 + Im(F)^2} \quad (3)$$

$$k_r = \sqrt{k_x^2 + k_y^2} \quad (4)$$

Lines were drawn along the curve where the amplitude decreased, and their slopes represented the average depth of the layer. The power spectrum $F(k)$ was obtained from the squared magnitude of the Fourier spectrum and averaged radially per wavenumber. This

power spectrum describes the distribution of gravitational anomaly energy as a function of spatial frequency $F(k) = \langle |F(k_x, k_y|^2 \rangle_{k=constant}$ For a gravity source at depth d, the Bouguer anomaly power spectrum follows an exponential relationship $F(k) \propto e^{-2kd}$ on a logarithmic scale, this relationship becomes linear. Ln $F(k) = -2kd +$ constant, the (-2*d*) is the linear slope of the plot of ln *F(k)* vs *k* used to estimate the depth *d*. Fourpot 1.3b software was employed to examine the radial power spectrum of the CBA dataset in the Lewa region.

Vertical and Horizontal Gradients

Vertical and horizontal derivatives define the edges of geological formations and source objects within gravitational or magnetic field maps [5]. A vertical derivative has been utilized to identify the edges of gravity-anomalous objects. This technique highlights geological features near the surface and enhances the spectrum wave components, where the zero value of the vertical gradient (VG) typically aligns with the geological boundary [13, 14]. The mathematical equations for the vertical gradients are as follows:

$$\mathrm{VG} = \frac{\partial \mathrm{g}}{\partial \mathrm{z}} \tag{5}$$

where *g* denotes the gravity anomaly. The horizontal gradient method evaluates the rate at which potential areas change along the *x*- and *y*-axes to identify subsurface structures [15]. Horizontal gradients help identify the boundaries of density or susceptibility contrasts in potential field data. Unlike the vertical gradient, which is only appropriate for shallow structures, this method is effective for detecting both shallow and deep sources [16, 17]. The total horizontal gradient (THG) of gravity data along the *x*- and *y-axes* can be represented as follows [18]:

$$\mathrm{THG}\ (x, y) = \sqrt{\left(\frac{\partial \mathrm{g}}{\partial \mathrm{x}}\right)^2 + \left(\frac{\partial \mathrm{g}}{\partial \mathrm{y}}\right)^2} \tag{6}$$

The CBA vertical and horizontal gradients were assessed, and regional and residual anomalies were distinguished. The residual anomaly was identified by subtracting the regional anomaly from CBA. Regional anomalies are attributed to deep, extensive structures, whereas residual anomalies are linked to shallow, smaller structures [19,20].

Tilt Angle Gradient

Derivative methods identify the horizontal boundary of gravity sources. Vertical derivatives enhance gravity field observations. The horizontal derivative and analytical signal amplitudes indicate the boundary. The Tilt angle (TA), introduced by Miller and Singh in 1994, identifies structural boundaries from varying depths [21]. TA contrasts the vertical and horizontal derivatives from -90° to 90°. Mathematically, the tilt angle equation can be obtained as [13, 14]:

$$\mathrm{TA} = \tan^{-1}\left(\frac{\mathrm{VG}}{\mathrm{HG\ (x,y)}}\right) \tag{7}$$

TA is positive over the source, zero at the boundary where the vertical derivative is zero and the horizontal derivative peaks, and negative outside the source [5,14].

The vertical and horizontal gradients and tilt angle calculations are presented in the frequency domain using a 2D FFT. In the Fourier domain, the gravity gradient equals the product of gravity and wavenumber in the derivative direction [22,23]. The Fourier transformation describes sinusoids and cosines at various spatial frequencies (k_x and k_y) [24].

Synthetic Model of Rectangular Prism

Before being applied to the high-resolution gravity field in the study area, we created a test model consisting of three pieces of rectangular prisms of a cylindrical (1), cube (2), and beam (3) to obtain a synthetic response to gravity anomalies and their gradients. The entire model was placed at the same depth of 500 m from the surface in the northwest direction (Figure 4a). The contrast of the density of the test model assumed a positive value of 0.43 gr/cm^3 (Figure 4b), resembling the intrusion pattern with a total area of 25 km^2.

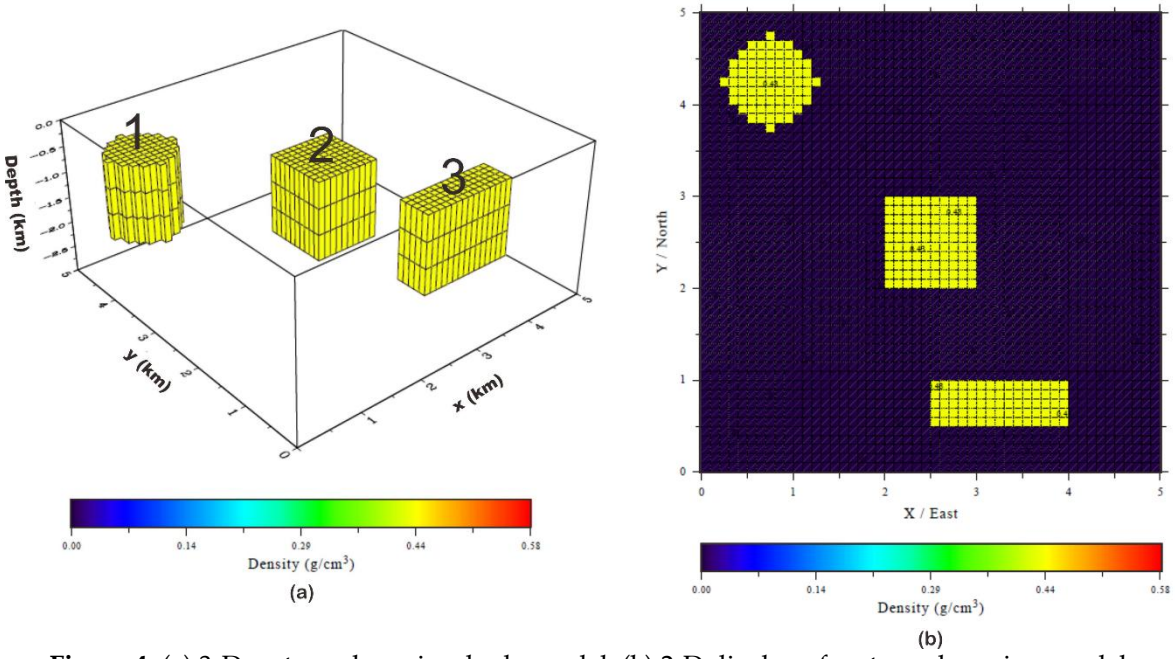

Figure 4. (a) 3-D rectangular prism body model; (b) 2-D display of rectangular prism model.

Furthermore, the theoretical response of the gravity field anomalies was determined through forward modeling and continued analysis of the vertical, horizontal, and tilt angle gradients using a 2-D fast Fourier transform (FFT). This synthetic test process was performed to obtain results as a control model when it was later applied to more complex field data. A synthetic gravity field anomaly response is positive between 0.18 mGal to 3.63 mGal, forming a circular pattern extending from northwest to southeast (Figure 5a). The highest anomaly is in the central part, caused by the cube object, whereas for the cylindrical and beam objects, it generally has moderate to low anomaly values.

The theoretical anomaly response shows the incorporation of specific anomalies by cube and beam objects such that the boundaries are not visible. To define the boundaries of anomalous objects, we performed vertical, horizontal, and tilt angle analyses using the FFT technique. The vertical gradient value generated from the test model ranged from -2,373 mGal/km to 4,945 mGal/km, with a pattern specific to the three models (Figure 5b). The anomaly in each object was visible to which the high contour indicated the source of the object, whereas the zero value was correlated with the border of the three objects. The horizontal gradient of the test object was typically more complex than the vertical gradient, ranging from 0.021 to 2.632 mGal/km (Figure 5c).

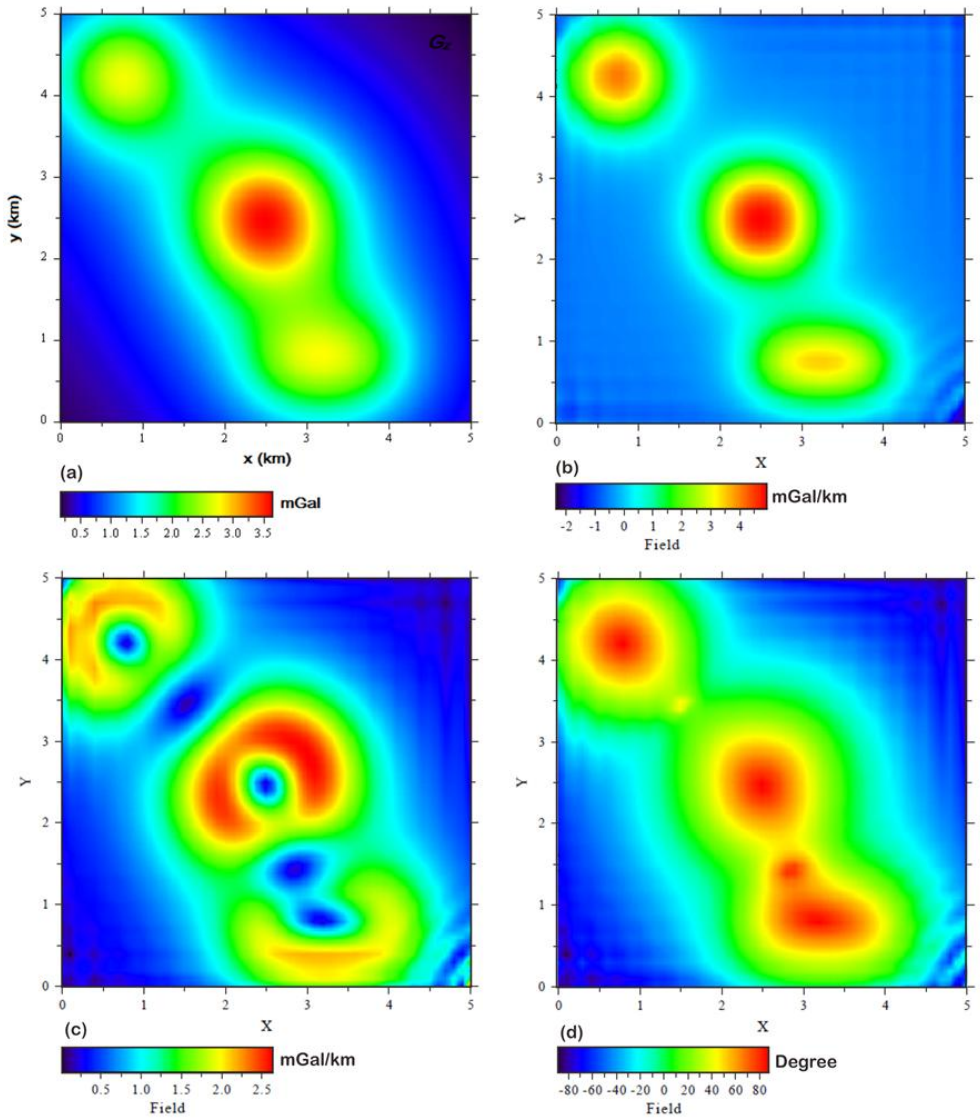

Figure 5. Forward modeling based on the 3-D prism model from Figure 4 (a) Gravity anomaly response; (b) Vertical gradient; (c) Horizontal gradient; (d) Tilt angle. Each model response provides specific information about the boundaries of the anomalous objects.

Low anomalies are generally related to the center of the source object, whereas high anomalies are correlated with the boundary of the object, although the test results have not been specifically observed. The Tilt angle is a comparison between the vertical and horizontal gradients. For these synthetic test models, the tilt angle ranges between -88.339° and 87.813°, with the high contour pattern on the source object causing anomalies and zero or near-zero contours associated with the third boundary of the object, although this is still not apparent owing to the merger of anomalies, while the negative contour is generally outside the source. The results of the synthetic test model were used as a control in the gradient analysis of high-resolution anomalous gravity data in the study area.

3D gravity data inversion

In this study, to facilitate the analysis of high-resolution gravity field gradients, we conducted three-dimensional inversion modeling on residual anomaly data following gravity anomaly

separation. The objective of this 3D inversion modeling is to acquire information regarding the density distribution of subsurface rocks in the Lewa district, East Sumba. Gravity modeling is an essential phase in gravity interpretation, focusing on identifying the density, depth, and shape of underground structures [25]. Inversion modeling used Grablox 1.7 and Bloxer 1.5. Grablox uses a three-dimensional block model where a rectangular superblock beneath the measurement area is divided into smaller elements with set density values [26]. BLOXER was used for visualization.

The inversion process optimizes block density to minimize differences between measured and calculated gravity data using linearized inversion with SVD and adaptive damping. After inversion, density variations enabled geological interpretation. The background density had a constant value subtracted from each minor block. The inversion uses Occam's method to minimize model roughness along with data error and uses a Lagrange multiplier to control data error against model smoothness [16], [24]. The process continues until iterations are complete and data differences become small. The root-mean-square (RMS) error measured the data. Four additional blocks at the model margin prevent boundary effects in the top computational layer. We performed 2D forward modeling on the residual gravity anomaly data to support the inversion results using GM-SYS on Oasis Montaj software, based on Talwani et al. (1959) [27] .

Result and Discussion

Complete Bouguer Anomaly in Lewa District, East Sumba

Table 2 presents the findings from the data verification of Earth's gravitational acceleration and the elevation of the gravity field models GGMplus and ERTM 2160. At Tambolaka Airport, the gravity field value determined from field measurements differed from that obtained using GGMplus by 0.16 mGal, whereas at Waingapu Airport, this difference was 12.87 mGal.

Table 2. Reference gravity station at Tambolaka and Waingapu Airport, Sumba Island, Nusa Tenggara Timur Province based on GGMplus and ERTM 2160.

No.	Airport	Latitude (Degree)	Longitude (Degree)	Elevation (m)	Gravity acceleration (mGal)
1	Tambolaka Waikabubak	-9.40000	119.40000	61.00	978287.70
2	Waingapu Mau Hau	-9.66667	120.30000	10.00	978308.00

The difference in the topography elevation value of the reference station with elevation from ERTM2016 in Tambolaka Airport at 12.8 m, while at Waingapu Airport by 2.2 m.

Based on the comparison of the data in Tables 1 and 2, there are differences or small variations between the gravity field data reference of the field measurements and the GGMplus-ERTM 2160 models so that the extracted gravity field data in the Lewa district located between the two airports are processed to obtain a complete Bouguer Anomaly.

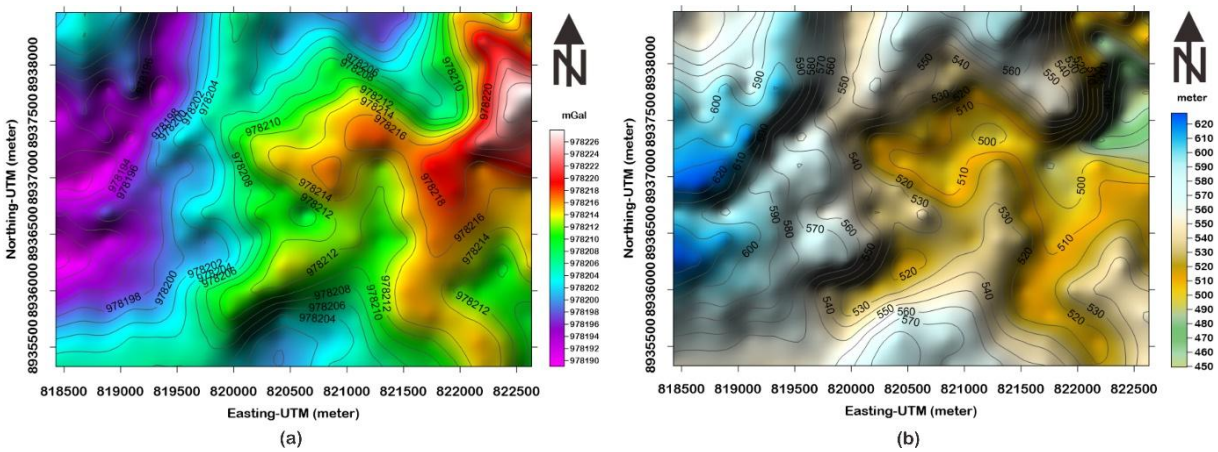

Figure 6. Earth's gravity field information for the Lewa district in the East Sumba regency, presented in UTM coordinates: (a) gravity acceleration data derived from GGMplus; (b) digital elevation data sourced from ERTM 2160.

The gravity acceleration value of the GGMplus model for the region of Lewa district ranges between 978189.0 mGal to 978228.2 mGal with a difference of 39.2 mGal. The pattern of the gravity field north-southeast with maximum acceleration is found in the east, while the minimum is found in the west (Figure 6a). The elevation value of the study area based on the DEM ERTM 2160 is between 448 m and 628 m above sea level, with a maximum value in the west and a minimum in the east, in the same direction as the Earth's gravitational acceleration (Figure 6b). This corresponds to the laws of Newton's gravity, which state that the value of the acceleration of gravity is always inversely proportional to the distance.

The correction of GGMplus gravity acceleration in the form of latitude and free air corrections generates free air anomalies in the research area ranging between 189.67 mGal – 205.78 mGal, northwest to the southeast, with high anomaly values extending from north to south in the eastern part, while low anomalies are found in the west (Figure 7a).

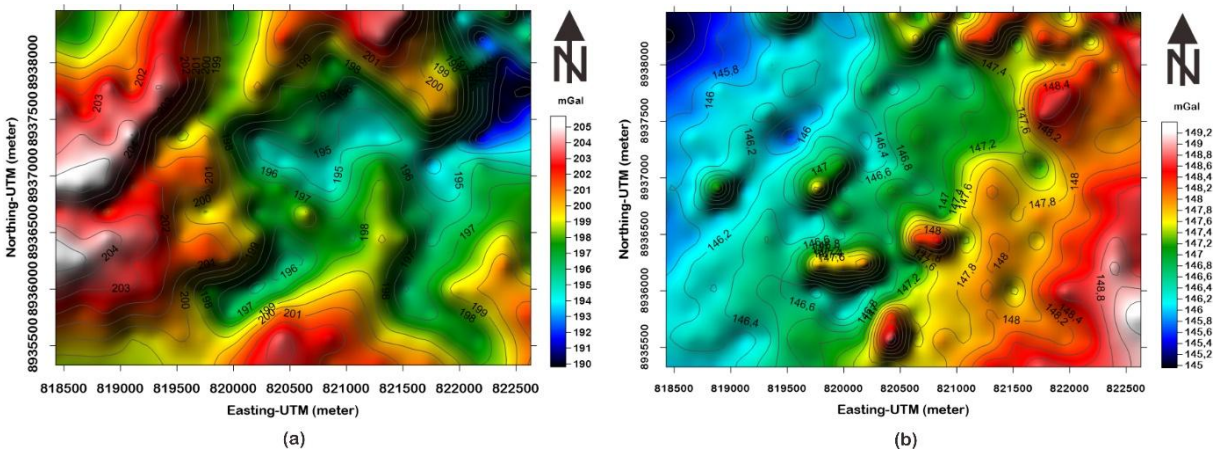

Figure 7. Data correction of the Earth's gravitational field in the Lewa District, East Sumba Regency: (a) free air anomaly; (b) Complete Bouguer anomaly.

In the Lewa District of East Sumba, the application of Bouguer and terrain corrections to the free-air anomaly data produced a complete Bouguer anomaly. This anomaly exhibits values ranging from 144.95 mGal to 149.43 mGal and displays more intricate feature trends compared to the free air anomalies (Figure 7b).

Significant anomalies with extended patterns were observed in the eastern study area, which diminished westward. The narrow range between the highest and lowest complete Bouguer anomaly values suggests that the area comprises similar rocks, mainly volcanic in nature. From the geological composite map of the Lewa area (Figure 1), it was found that the distribution of metal mineral zones is generally associated with silicification rocks [2] related to high-gravity anomalies in a circular form in some locations on the complete Bouguer anomaly map.

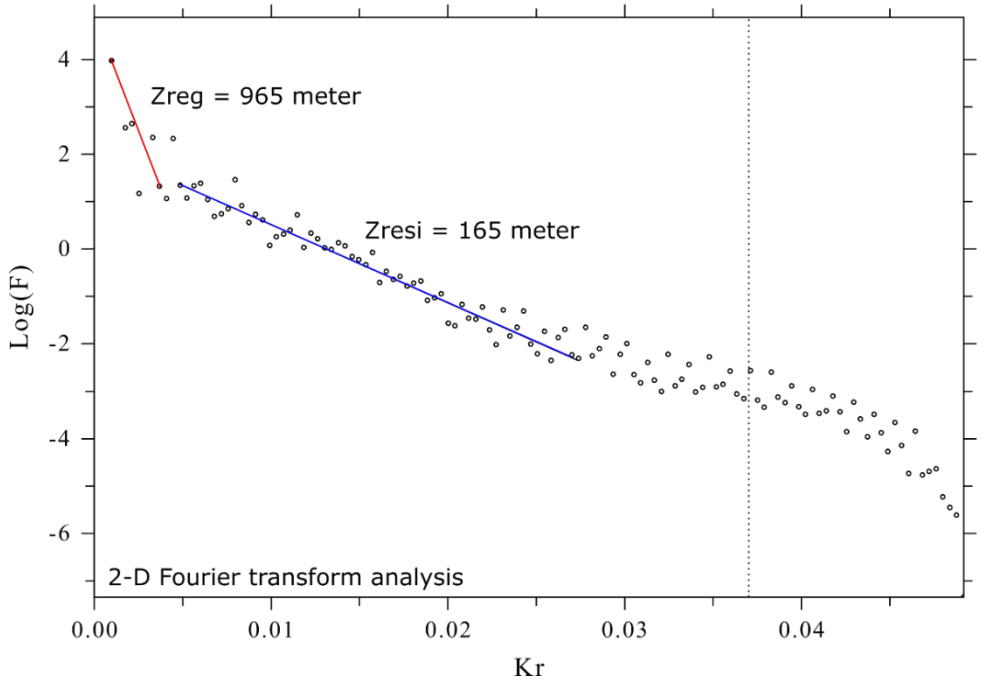

Figure 8. The radial average amplitude spectrum of the complete Bouguer anomaly in the Lewa region is shown. Each radial wave section has line segments with two distinct slopes (Z_{reg} and Z_{resi}) fitted to it.

Additionally, we conducted a two-dimensional radial spectrum analysis on the CBA data from the Lewa region to determine the window width and depths of both the shallow (residual) and deep (regional) anomalies (Figure 8). Essentially, spectrum analysis is performed by applying Fourier transform to the determined anomaly data. The results of the spectrum analysis show that the estimated average depth associated with the regional anomaly (Z_{reg}) is 965 meters, while the estimated average depth associated with the residual anomaly (Z_{resi}) is 165 meters (Figure 8).

Regional and Residual Anomalies in Lewa District

The potential for metal minerals in the study area is limited and is not represented in the complete Bouguer anomaly map. Consequently, separating the residual and regional anomalies is essential to better delineate the mineral potential boundaries of the geological

structure. We employed low-pass filtering to extract regional anomalies, with residuals derived from the difference between the complete Bouguer and regional anomalies. The regional anomalies were positive, ranging from 145.057-149.178 mGal, extending northwest to southeast, with the minimum value in the west increasing eastward (Figure 9a).

Residual anomalies are more complex than Bouguer and regional anomalies. Anomaly values ranged from -0.741 to 1.087 mGal, with maximum spots in mid-and northeastern areas (Figure 9b). This maximum value is allegedly associated with geological structures identified as potential metal minerals in Lewa.

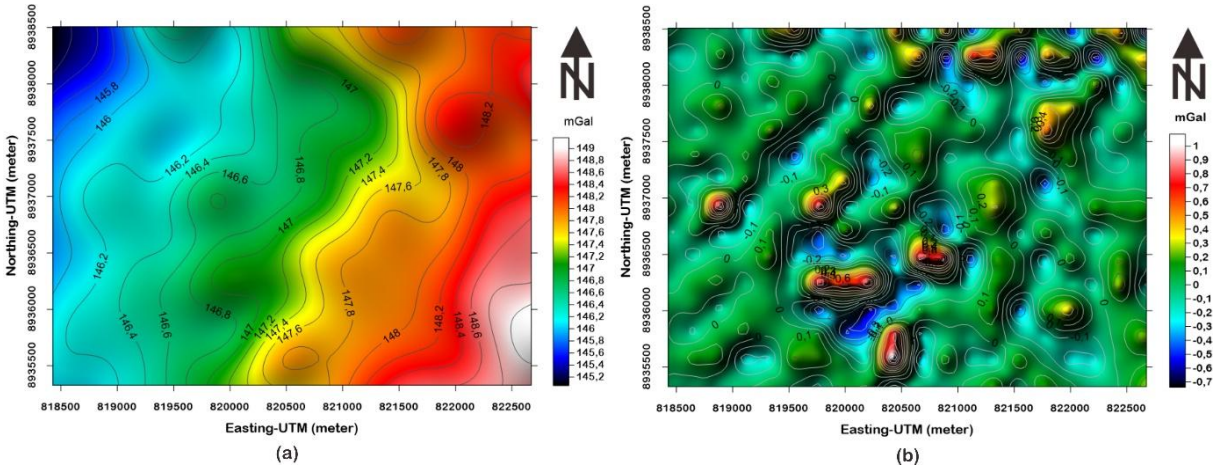

Figure 9. Distinction between regional and residual anomalies in the Lewa district of the East Sumba regency: (a) regional anomaly; (b) residual anomaly.

To emphasize this assumption, we overlaid the map of the residual gravity anomaly with the geological structure and mineral extension shown in Figure 1, as shown in Figure 10. This results in a better description of the existence of fault systems correlated with low residual anomaly values. This low value is usually associated with a weak or fractured zone with low rock density owing to tectonic activity in the research location. The estimation of geological structures as potential metal minerals is shown in five (5) segments (dashed red circles) with high positive anomalous dominance.

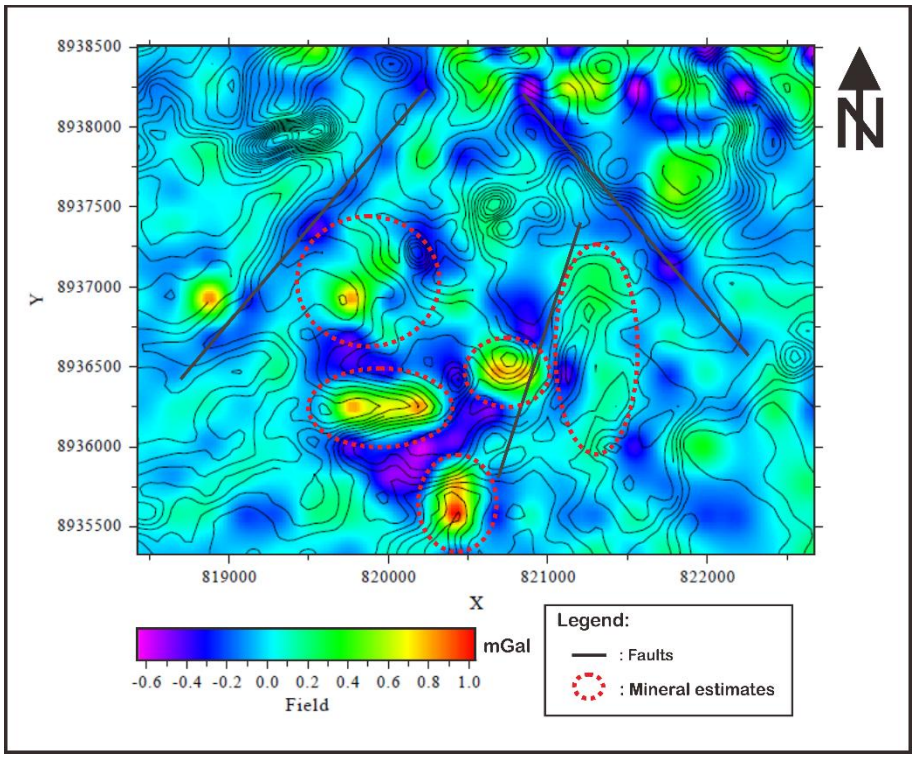

Figure 10. Identification of the fault and mineral potential of metals in the district of Lewa, East Sumba Regency, on the residual gravity anomaly. The high residual gravity anomaly correlates with metal minerals.

The Gradient Anomalies in Lewa District

To determine the boundaries of anomalous sources and geological structures indicating metal minerals in the Lewa district of the East Sumba Regency, an analysis of vertical and horizontal gradients and tilt angles was conducted. The vertical gradients ranged from negative to positive, between -0.011 mGal/m and 0.017 mGal/m (Figure 11a). The vertical gradient map reveals fault structures and geological contacts associated with zero values. While the metal mineral potential in Lewa is not directly visible on the vertical gradient map, it is believed to be linked to the maximum gradient value.

The horizontal gradients have positive values from 3.68.10-6 mGal/m to 0.0112 mGal/m. On this map, the boundaries of the structure or causative source outline related to the potential of metal minerals were detected using the maximum amplitude value (Figure 11b). Edge borders are not visible on the residual anomaly and vertical gradient maps but are clearly visible and interconnected on the horizontal gradient map. The continuity of the faulting structure is not visible in this section.

The tilt angle ranged from -89.931° to 89.003°, with positive anomalies dominating the study area (Figure 11c). The boundaries of the geological structure, particularly the fault, appear very clear on the tilt angle map, corresponding to zero or near-zero values. The zero contours of the tilt angle are generally located close to the boundary of the causative body [21, 28]**.** The potency of the metal minerals in Lewa was identified with a high positive value for the tilt angle anomaly as a source of anomalies, either shallow or deep. Furthermore, qualitative

interpretation results in the form of vertical and horizontal gradient analyses as well as a tilt angle that will be used as a constraint in the quantitative modeling of subsurface density in the Lewa district, East Sumba.

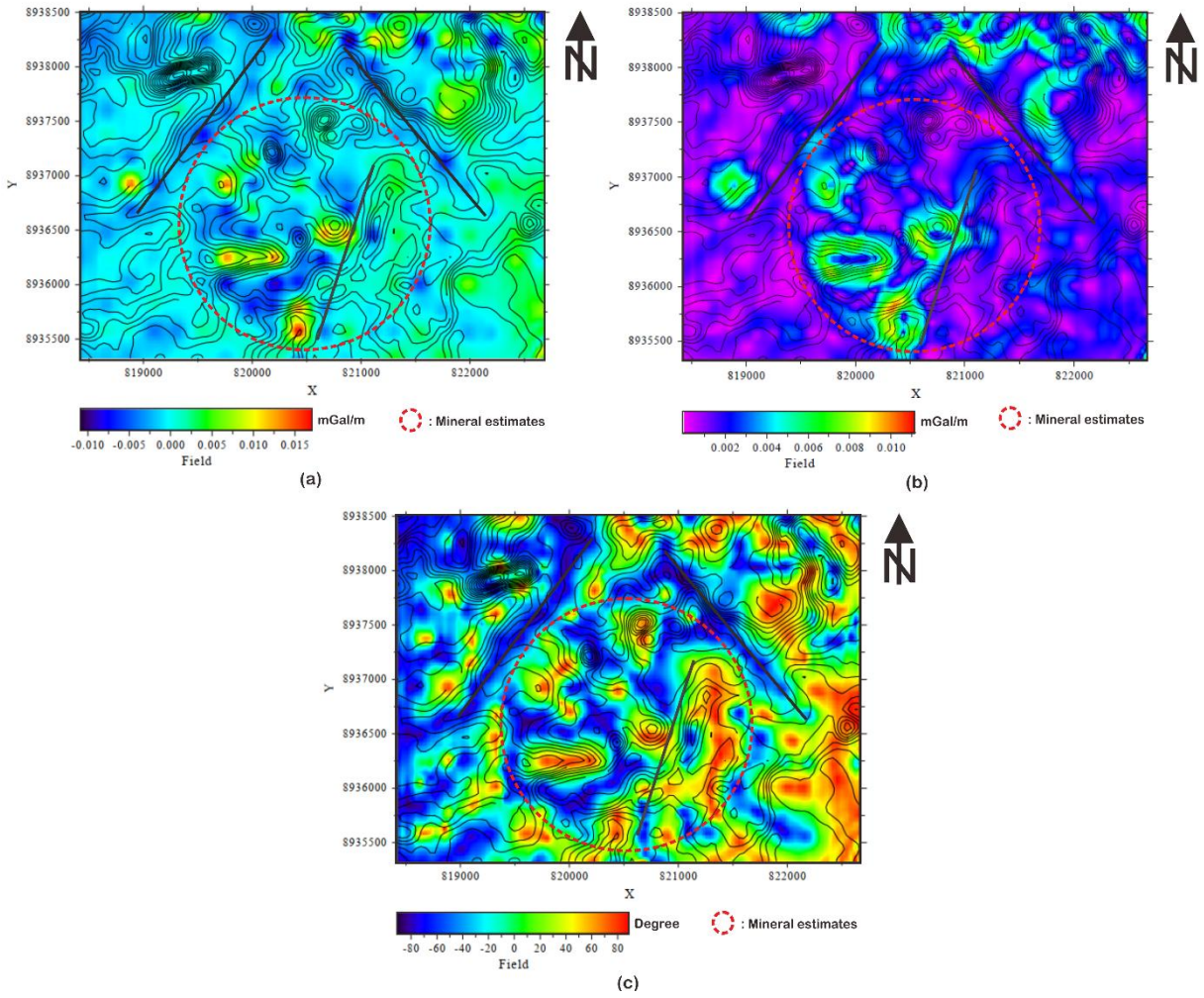

Figure 11. Gravity gradient analysis of the complete Bouguer anomaly in the Lewa district, East Sumba Regency: (a) vertical gradient; (b) Horizontal Gradient; (c) tilt angle. In general, mineral identification is associated with medium to high values, whereas faults are associated with low values.

Density Distribution in Lewa District, East Sumba

A three-dimensional model of subsurface density distribution in the Lewa district, East Sumba regency, is illustrated through a series of cross sections. These cross-sections consisted of three incisions, labeled A-A', B-B', and C-C', each positioned perpendicular to the fault line. The density distribution model of cross-section A-A', extending from southeast to northwest, was integrated with 2.5 D modeling and the results of the vertical and horizontal gradient analyses (Figure 12). The vertical gradient analysis showed a zero value, indicating the contact boundary and the characteristics and location of the geological structures. In contrast, the horizontal gradient analysis revealed minimum and maximum values, marking the contact boundary between rock formations. Both analyses suggest the presence of a fault system interpreted as an ascending fault.

The cross-section A-A' spans 978 m and traverses two rock formations: the Waikabubak Formation, composed of limestone, claystone, passive marl inserts, and tuffanic marl with an estimated density ranging from 2.62 g/cm³ to 2.67 g/cm³, and the Masu Formation, which includes an andesitic-basaltic volcanic rock unit with an estimated density of 2.7 g/cm³ and a silicified rock unit with a density of 2.77 g/cm³ [2]. To enhance the 2D forward model, perpendicular cuts were applied to the 3D residual gravity anomaly inversion model. In this context, the lower density value of approximately 2.6 g/cm³ is interpreted as the Waikabubak Formation, situated between the higher density value of about 2.71 g/cm³, interpreted as the Masu Formation, and the suspected fault. Overall, the results of these two models corroborate each other.

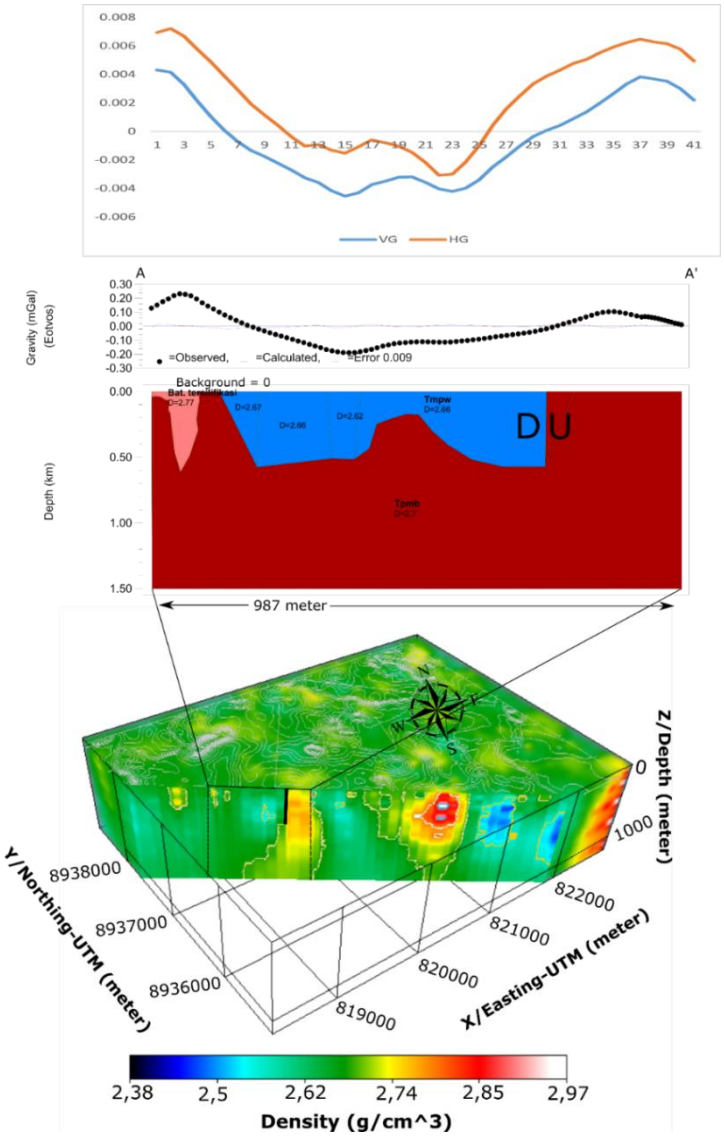

Figure 12. Subsurface density distribution model of incision A-A' from 3D inversion modeling of gravity anomalies combined with forward modeling and horizontal-vertical gradient analysis.

The 2D model for cross-section B-B' along 787 m from southwest to northeast intersects the Waikabubak Formation, comprising limestone, clay limestone, passive marl inserts, and

tuffanic marl with density between 2,6 - 2.68 g/cm^3, the Masu Formation of andesitic-basaltic volcanic rock units with density of 2.7 - 2.75 g/cm^3, and silicified rock units with density of 2.8 g/cm^3 (Figure 13). To validate the 2D model, a 3D gravity inversion model was used the 2D model. The model shows a significant density contrast. The shifting system occurs in the Masu Formation (2.7 g/cm^3) moving upward, causing faulting. The fault section was sedimented by the Waikabubak Formation (2.57 g/cm^3).

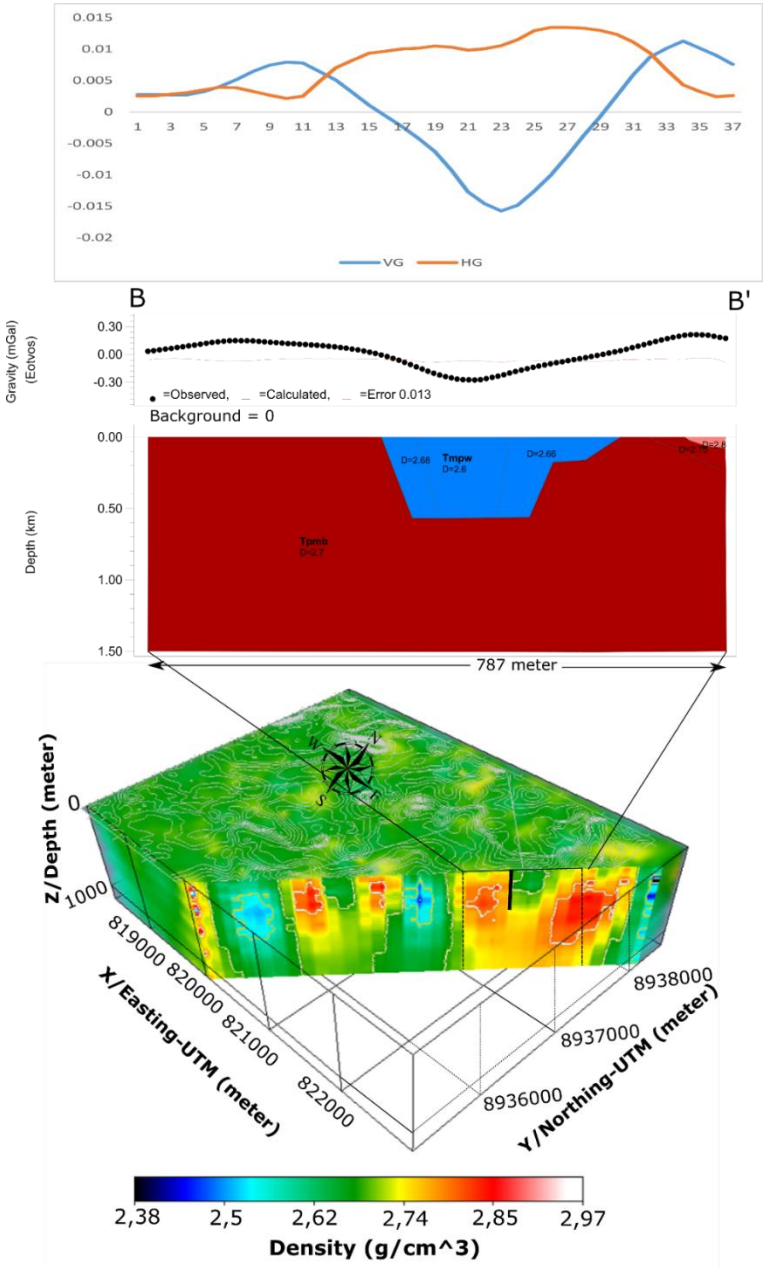

Figure 13. Subsurface density distribution model of incision B-B' from 3D inversion modeling of gravity anomalies combined with forward modeling and horizontal-vertical gradient analysis.

The modeling results align with the horizontal gradient analysis, showing minimum and maximum values indicating rock contact boundaries, while the vertical gradient analysis

shows a zero value at contact boundaries and characteristics of the suspected ascending fault structure. Cross-section 2D C-C' is 1044 m long and runs northwest to southeast across the two rock formations. The Waikabubak Formation consists of limestone, claystone, passive marl, and tuffan marl inserts, with a density range between 2.5 g/cm^3 and 2.67 g/cm^3. Meanwhile, the Masu Formation consists of andesitic-basaltic volcanic rock units with densities ranging from 2.7 g/cm^3 to 2.75 g/cm^3, and silicified rock units with a density of 2.8 g/cm^3 (Figure 14). The horizontal and vertical gradient analysis shows a fault zone that is interpreted as a thrust fault.

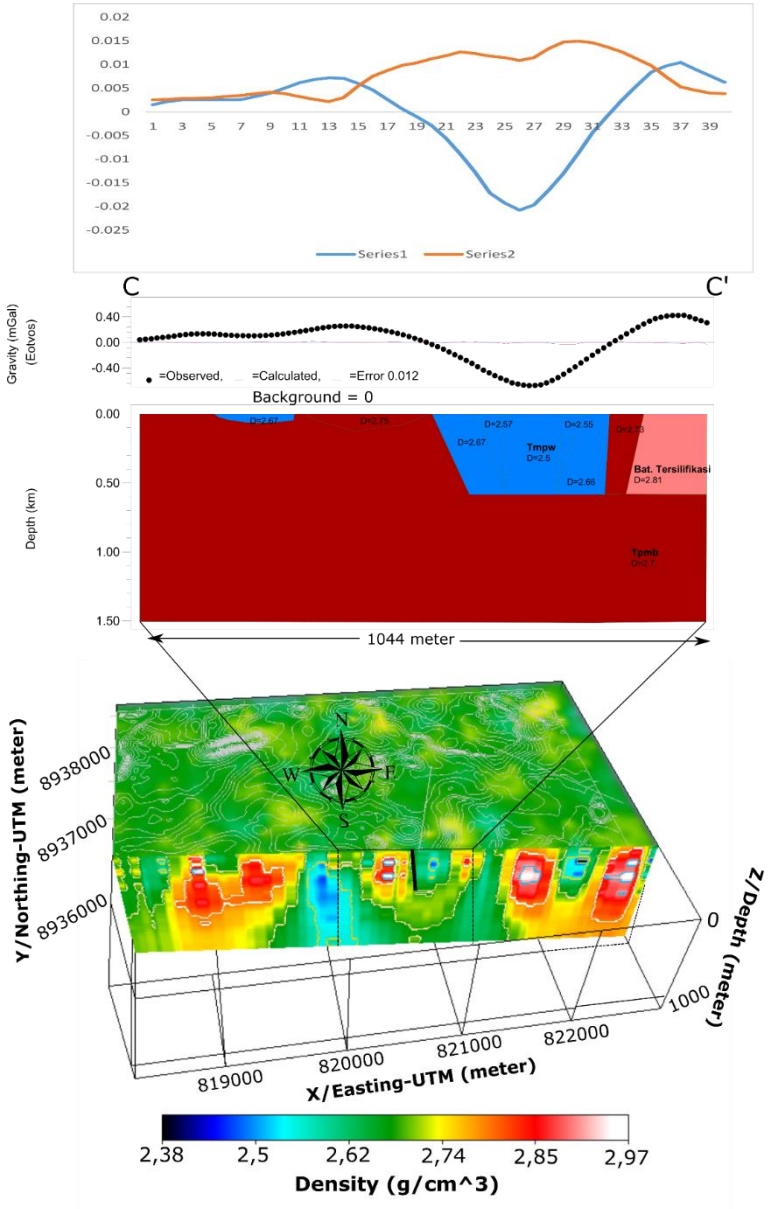

Figure 14. Subsurface density distribution model of incision C-C' from 3D inversion modeling of gravity anomalies combined with forward modeling and horizontal-vertical gradient analysis.

For the 3D incision, gravity inversion was performed to emphasize the 2D model results by cutting the model according to the incision of the 2D model. From the model obtained, there

is good agreement between the 3D and 2D model incisions, where there are low-density values among higher densities. The higher density is identified as the hanging wall (2.71 gr/cm^3), while the lower density (2.60 gr/cm^3) is interpreted as the foot wall. This was due to the sedimentation process in the foot wall area. Higher density values indicate more complex and massive rocks, thus identified as the Masu Formation, while rocks with lower density tend to indicate easier rocks, thus identified as the Waikabubak Formation.

Compared to alternative geophysical methodologies, the gradient approach and three-dimensional gravity inversion offer distinct advantages for this study. This cost-effective, high-resolution satellite gravity data-based method is particularly suitable for early stage mineral exploration in remote and data-deficient regions, such as Lewa. Gravity gradient analysis facilitates high-resolution structural delineation at a minimal expense. Its sensitivity to subtle density variations enables precise mapping of fault contacts and intrusion boundaries, which are critical factors in mineralization. Other geophysical techniques, such as magnetic surveys, may fail to detect non-magnetic mineral targets, whereas seismic surveys encounter logistical challenges in the complex terrain of East Sumba.

Conclusion

Utilizing high-resolution gravity field data from GGMplus and ERTM 2160 offers valuable insights into the distribution of metal minerals in the Lewa District of the East Sumba Regency. Adjustments to the GGMplus and ERTM 2160 gravity models resulted in a complete Bouguer anomaly that was aligned with the geological conditions of the study area. A preliminary qualitative interpretation employing gradient or derivative analysis of the vertical, horizontal, and tilt angles of gravity anomalies has enhanced the visibility of the boundaries of anomaly sources or faulting structures in the Lewa region. This is characterized by a zero- or maximum-value correlation with the gradient contour of gravity. The potential of metal minerals is generally associated with the maximum gradient value of vertical, horizontal, or tilt angles. In the tilt angle map, the predominance of highly positive contours across the region was attributed to the influence of volcanic rock serving as a basement in Lewa, East Sumba. Earth gravity modeling in the study area provides an estimate of the thrust fault system, with the maximum and minimum vertical gradient values indicating the contact plane boundary. Cross-sections A-A', B-B', and C-C' of the subsurface 2D model are dominated by volcanic rocks of the Masu Formation, whereas the broken section is filled by sedimentary rocks associated with the Waikabubak Formation and silicified rocks caused by igneous intrusion. The 3D gravity inversion model with a range of density values from 2.22 g/cm^3 to 2.97 g/cm^3 indicates the presence of rock intrusion at a depth of 215 m, which is thought to be the main factor in the formation of metallic minerals in the study area. Fault structures are thought to result from the intrusion of more massive igneous rocks into softer rocks, while mineralization in the study area is strongly associated with activity and changes caused by tectonic activity. Consequently, gravity gradient and 3D inversion modeling techniques present strategically advantageous options for preliminary mineral exploration in geologically intricate and data-deficient regions.

Acknowledgment

We thank Curtin University for providing the GGMplus and ERTM 2160 Earth gravity field models and software extraction at no cost for this research. I also thank Mr. Pirtijarvi for creating the Fourpot, Grablox, and Bloxer software, which uses FFT to examine Earth's Gravity Gradient Components, and for offering complimentary 3D inversion modeling of Earth's gravity anomalies.

References

[1] Zulfikar, T., T. Sutisna, dan M. Supardan. Inventarisasi dan Evaluasi Mineral Non Logam di Kabupaten Sumba Barat dan Sumba Timur, Provinsi Nusa Tenggara Timur. Bandung: Direktorat Sumber Daya Mineral, 2004. https://geologi.esdm.go.id/perpustakaan?p=show_detail&id=6892.

[2] Tim Prospeksi. Laporan Prospeksi Mineral Logam di Kabupaten Sumba Timur, Provinsi Nusa Tenggara Timur. Bandung: Kementerian Energi dan Sumber Daya Mineral, 2011. https://geologi.esdm.go.id/perpustakaan?p=show_detail&id=2583.

[3] J. Yan, Q. Lu, F. Luo, S. Cheng, K. Zhang, Y. Zhang, Y. Xu, C. Zhang, Z. Liu, S. Ruan, X. Wang, "A gravity and magnetic study of lithospheric architecture and structures of South China with implications for the distribution of plutons and mineral systems of the main metallogenic belts," *J. Asian Earth Sci.*, vol. 221, p. 104938, Nov. 2021.

[4] M. O. zgu Arısoy and Ü. Dikmen, "Potensoft: MATLAB-based software for potential field data processing, modeling and mapping," *Comput. Geosci.*, vol. 37, no. 7, pp. 935–942, Jul. 2011.

[5] A. Eshaghzadeh, A. Dehghanpour, and R. A. Kalantari, "Application of the tilt angle of the balanced total horizontal derivative filter for the interpretation of potential field data," *BGTA*, vol. 59, no. 2, pp. 161–178, 2018.

[6] C. Hirt, S. Claessens, T. Fecher, M. Kuhn, R. Pail, and M. Rexer, "New ultrahigh-resolution picture of Earth's gravity field: NEW PICTURE OF EARTH'S GRAVITY FIELD," *Geophys. Res. Lett.*, vol. 40, no. 16, pp. 4279–4283, Aug. 2013.

[7] C. Hirt, M. Kuhn, S. Claessens, R. Pail, K. Seitz, and T. Gruber, "Study of the Earth's short-scale gravity field using the ERTM 2160 gravity model," *Comput. Geosci.*, vol. 73, pp. 71–80, Dec. 2014.

[8] Y. L. Ekinci and E. Yiğitbaş, "Interpretation of gravity anomalies to delineate some structural features of Biga and Gelibolu peninsulas, and their surroundings (north-west Turkey)," *Geodin. Acta*, vol. 27, no. 4, pp. 300–319, Oct. 2015.

[9] P. Sumintadireja, D. Dahrin, and H. Grandis, "A Note on the Use of the Second Vertical Derivative (SVD) of Gravity Data with Reference to Indonesian Cases," vol. 50, no. 1, pp. 127–139, 2018.

[10] G. De Gelder, T. Solihuddin, D. Amanda Utami, M. Hendrizan, R. Rachmayani, D, Chauveau, C. Authemayou, L. Husson, S. Yudawati Cahyarini, "Geodynamic control on Pleistocene coral reef development: Insights from northwest Sumba Island (Indonesia)," *Earth Surf. Process. Landf.*, vol. 48, no. 13, pp. 2536–2553, Oct. 2023.

[11] M. C. Dentith and S. T. Mudge, *Geophysics for the mineral exploration geoscientist*. Cambridge, United Kingdom: Cambridge University Press, 2014.

[12] E. Balkan and M. Tün, "Use of Land Gravity Data in Small Areas to Support Structural Geology, a Case Study in Eskişehir Basin, Turkey," *Appl. Sci.*, vol. 13, no. 4, p. 2286, Feb. 2023.

[13] R. Lewerissa, Sismanto, and L. A. S. Lapono, "Identification of sediment–basement structure in West Papua province, Indonesia, using gravity and magnetic data inversion as an Earth's crust stress indicator," Acta Geophys., vol. 71, no. 1, pp. 209–226, Sep. 2022.

[14] I. M. Ibraheem, M. Haggag, and B. Tezkan, "Edge Detectors as Structural Imaging Tools Using Aeromagnetic Data: A Case Study of Sohag Area, Egypt," *Geosciences*, vol. 9, no. 5, p. 211, May 2019.

[15] M. Hicheri, B. Ramdhane, S. Yahyaoui, and T. Gonenc, "New Insights from Gravity Data on the Geodynamic Evolution of Northern African Passive Margin, Case Study of the Tajerouine Area (Northern Tunisian Atlas)," *J. Geol. Geophys.*, vol. 08, no. 01, 2018.

[16] J. Abderbi, D. Khattach, and J. Kenafi, "Multiscale analysis of the geophysical lineaments of the High Plateaus (Eastern Morocco): structural implications," J. Mater. Environ. Sci., vol. 8, pp. 467–475, 2017.

[17] R. Lewerissa, S. Sismanto, A. Setiawan, and S. Pramumijoyo, "The igneous rock intrusion beneath Ambon and Seram islands, eastern Indonesia, based on the integration of gravity and magnetic inversion: its implications for geothermal energy resources," *Turk. J. EARTH Sci.*, vol. 49, no. 4, pp. 596–616, May 2020.

[18] L. T. Pham, K. Abdelrahman, Da. Viet Nguyen, D Gomez-Ortiz, N. Ngoc Long, L. Duc Luu, T. Duc Do, Q. Thanh Vo, T. Thi Nguyen, H. Thi Nguyen, A. Eldosouky, "Enhancement of the balanced total horizontal derivative of gravity data using the power law approach," Geocarto International, vol. 39, no. 1, p. 2335251, Jan. 2024.

[19] J. Nouraliee, S. Porkhial, M. Mohammadzadeh-Moghaddam, S. Mirzaei, D. Ebrahimi, and M. R. Rahmani, "Investigation of density contrasts and geologic structures of hot springs in the Markazi Province of Iran using the gravity method," Russ. Geol. Geophys., vol. 56, no. 12, pp. 1791–1800, Dec. 2015.

[20] M. Mohammadzadeh Moghaddam, S. Mirzaei, J. Nouraliee, and S. Porkhial, "Integrated magnetic and gravity surveys for geothermal exploration in Central Iran," Arab. J. Geosci., vol. 9, no. 7, p. 506, Jun. 2016.

[21] Z. Chen, L. Mou, and X. Meng, "The horizontal boundary and top depth estimates of buried source using gravity data and their applications," *J. Appl. Geophys.*, vol. 124, pp. 62–72, Jan. 2016.

[22] K. L. Mickus and J. H. Hinojosa, "The complete gravity gradient tensor derived from the vertical component of gravity: a Fourier transform technique," J. Appl. Geophys., vol. 46, no. 3, pp. 159–174, Mar. 2001.

[23] H. Grandis and D. Dahrin, "Full Tensor Gradient of Simulated Gravity Data for Prospect Scale Delineation," vol. 46, no. 2, pp. 107–124, 2014.

[24] M. Pirttijarvi, FOURPOT: Potential field data processing and analysis using 2-D Fourier transform, User's guide to version 1.3b, Department of Physics, University of Oulu, Finland, 2014. https://sites.google.com/view/markkussoftware/gravity-and-magnetic-software/fourpot.

[25] M. Abdel Zaher, H. Saibi, K. Mansour, A. Khalil, and M. Soliman, "Geothermal exploration using airborne gravity and magnetic data at Siwa Oasis, Western Desert, Egypt," *Renew. Sustain. Energy Rev.*, vol. 82, pp. 3824–3832, Feb. 2018.

[26] H. Saibi, S. Mogren, M. Mukhopadhyay, and E. Ibrahim, "Subsurface imaging of the Harrat Lunayyir 2007–2009 earthquake swarm zone, western Saudi Arabia, using potential field methods," *J. Asian Earth Sci.*, vol. 169, pp. 79–92, Jan. 2019.

[27] S. B. Babu, A. V. Satyakumar, A. V. Kulkarni, and P. K. Vats, "Structurally controlled mineralization in parts of Aravalli craton, India: Constraints from gravity and magnetic data," *J. Geodyn.*, vol. 155, p. 101954, Mar. 2023.

[28] S. A. Hosseini, N. Keshavarz Faraj Khah, P. Kianoush, Y. Arjmand, A. Ebrahimabadi, and E. Jamshidi, "Tilt angle filter effect on noise cancelation and structural edges detection in hydrocarbon sources in a gravitational potential field," Results in Geophysical Sciences, vol. 14, p. 100061, Jun. 2023.